Hybrid smart actuator combining electroactive polymers with superelastic TiNiCuCo

Benjamin Zemlin*[a], Julian Kunze[a], Bobby Cozette[b], Sabrina Curtis[b], Stefan Seelecke[a], Eckardt Quandt[d], Paul Mozki [e]
[a]intelligent Materials System Lab, Saarland University, Saarbrücken; [b]Khanjur R&D, LLC Silver Spring, MD, 20903 USA; [c]Christian-Albrechts-Universität zu Kiel Kiel; [d]Zentrum für Mechatronik und Automatisierungstechnik gGmbH, Saarbrücken

ABSTRACT

This paper presents a novel approach to smart actuation by integrating structured superelastic shape memory alloy (SMA) thin-films as electrodes in dielectric elastomer actuators (DEAs), advancing the field of smart material actuation. Traditional DEAs utilize electrodes with embedded conductive particles, such as carbon black, in polydimethylsiloxane (PDMS), which often have low conductivity. By employing TiNiCuCo thin-film electrodes, this study significantly enhances conductivity. Additionally, the auxetic structure and superelastic properties of these films are leveraged to achieve polymer-compliant low stiffness, large deformation, and necking prevention. The research demonstrates that these structured metallic electrodes, originally designed for flexible electronics, are effective in DEAs, despite not being specifically designed for this application. Through detailed electro-mechanical characterization, including actuation experiments, we validate the functionality of the hybrid SMA-DEA technology. The results highlight the potential for smart self-sensing by monitoring capacitance changes due to deformation and deformation through applying voltages to the SMA-DEA hybrid actuator. Future work will focus on optimizing the auxetic structure and incorporating mechanical biasing into the structure of the TiNiCuCo electrodes, to further miniaturize the system. This integration paves the way for high-performance, compact, and versatile smart actuators suitable for various advanced applications, such as smart wearable devices and ultrasound emitters.

Keywords: EAP, SMA, Hybrid, DET, TiNiCuCo

1. INTRODUCTION

Dielectric elastomer transducers (DETs) have attracted considerable attention as a promising class of electroactive polymers for soft actuation. DETs typically consist of a thin dielectric elastomer, commonly silicone or acrylic [1], sandwiched between two compliant electrodes. When a high voltage is applied, an electric field is established across the elastomer, generating a Maxwell stress (1) that compresses the film in thickness and causes a lateral expansion governed by the Poisson ratio. This mechanism enables large, reversible deformations and high-frequency responses, making DETs ideal for applications in robotics, adaptive optics, and wearable devices.

$$\sigma_{\mathrm{M}} = \varepsilon_0 \varepsilon_r \left(\frac{U}{z}\right)^2 \tag{1}$$

Despite these attractive properties, DET performance is strongly dependent on the properties of the electrodes. Traditional electrodes, such as carbon black (CB) particles embedded in a polydimethylsiloxane (PDMS) matrix, are widely used due to their flexibility and ease of processing [2]. However, their relatively high electrical resistance—in the kilohm range—limits the efficiency of energy transfer, especially in high-frequency applications where rapid charging and discharging are required [3]. In contrast, metallic electrodes can offer significantly lower resistance. However, achieving sufficient elastic deformation in nonstructured metal films is challenging because most metals exhibit an elastic strain of less than 1% [4].

Shape memory alloys (SMA), such as nickel–titanium (NiTi) alloys, are known for their shape memory effect and superelastic behavior, which result from reversible martensitic transformations [5]. This transformation enables SMAs to recover predefined shapes upon heating and to undergo large, reversible strains—up to approximately 8%—through stress-

Electroactive Polymer Actuators, Sensors, and Devices (EAPAD) 2025, edited by Stefan S. Seelecke, Anne Ladegaard Skov, Kentaro Takagi, John D. W. Madden, Proc. of SPIE Vol. 13431, 134310H
2025 Published by SPIE · 0277-786X · doi: 10.1117/12.3051443

induced phase changes. SMA actuators, relying on the shape memory effect, exhibit high energy density and mechanical robustness, although their response is traditionally limited by slow thermal activation. Recent developments in the processing of superelastic SMA thin-films, have led to the fabrication of freestanding SMA electrodes capable of ultra-low fatigue behavior under deformation [6]. The stretchability can be further increased by structuring the thin-films [7]. Especially auxetic structures are promising. These auxetic structures, characterized by a negative Poisson's ratio, enhance mechanical compliance and prevent necking under tensile loads, thereby optimizing the deformation behavior.

The integration of DETs with freestanding, structured SMA electrodes presents an exciting opportunity to merge the high-frequency, large-stroke actuation of dielectric elastomers with the superior electrical conductivity and mechanical stability of SMAs. In our work, we introduce a hybrid smart transducer system that employs 50 µm thick structured superelastic TiNiCuCo thin-films (SSTTFs) as compliant electrodes on a silicone-based DET. These SSTTFs, originally designed for flexible electronics [8], are produced via a process combining photolithography, DC magnetron sputtering, and wet chemical etching to release the thin-film from a silicon wafer [7]. Subsequent annealing at 700°C for 15 minutes yields a film with an austenite finish temperature of –9°C, ensuring superelastic behavior at room temperature [7].

2. EXPERIMENTAL

The goal of this work is the characterization of the electrical properties of the novel hybrid SMA-DET structure. The analysis includes capacitance and resistance measurements to evaluate the electrodes' suitability for (self-)sensing and efficient electrical conduction for efficient operation.

Preparation of Actuator Samples

Both actuator types in this study feature an active area of 11 mm × 11 mm to allow direct performance comparisons. A 50 µm thick Wacker Elastosil 2030 silicone film serves as the dielectric elastomer and is fixed in a metal frame without pre-stretch.

PDMS+CB Electrode Samples

For the PDMS+CB electrodes, a paste containing carbon black, PDMS, and solvents is screen-printed onto the silicone film as 15 mm long by 11 mm wide strips and subsequently cured. The electrode strips are offset to create an 11 mm overlap forming the active area, with protruding ends serving as electrical contacts. Prior to cutting, 11 mm wide Kapton tape is applied on opposing sides of the silicone film to stabilize the DET and prevent the film from flipping and self-adhering. Finally, the DEA is cut as a 14 mm wide strip, leaving 1.5 mm wide insulation edges to prevent sparking at high voltages - an aspect particularly critical for the TiNiCuCo electrode samples.

TiNiCuCo Electrode Samples

Freestanding 50 µm thick SSTTFs are fabricated via photolithography, sputtering, and wet chemical etching to release the SMA thin-film from the silicon wafer (see Lima de Miranda et al. [9]). The wafers are annealed at 700°C for 15 minutes, resulting in an austenite finish temperature of –9°C and room-temperature superelasticity. A schematic of the preparation of the DET employing the TiNiCuCo electrodes is shown in Figure *1*. First the hexagonal structures are cut from the wafer (see Figure *1* a))). Then the wafers are cut into 11 mm wide strips using a scalpel (b). Prior to electrode placement, Kapton tape is applied to the silicone film, and two 11 mm wide strips are positioned in parallel, leaving an 11 mm gap (c)). The first electrode is aligned on the film using printed markings, and the frame is mounted so that the electrode is on top of the film. The second electrode is positioned underneath the silicone film.Proper alignment is assured with the help of a mikroscope via backlighting and a micrometer translation stage (d)). Finally, the second electrode is pressed onto the underside of the silicone film, adhering without additional adhesive.The finished DET is clamped into the Experimental setup as shown in e) and f). In 5) the Kapton tape is excluded for better visibility of the SSTTF electrode, whereas f) is a schematic of a side view of the clamped DET.

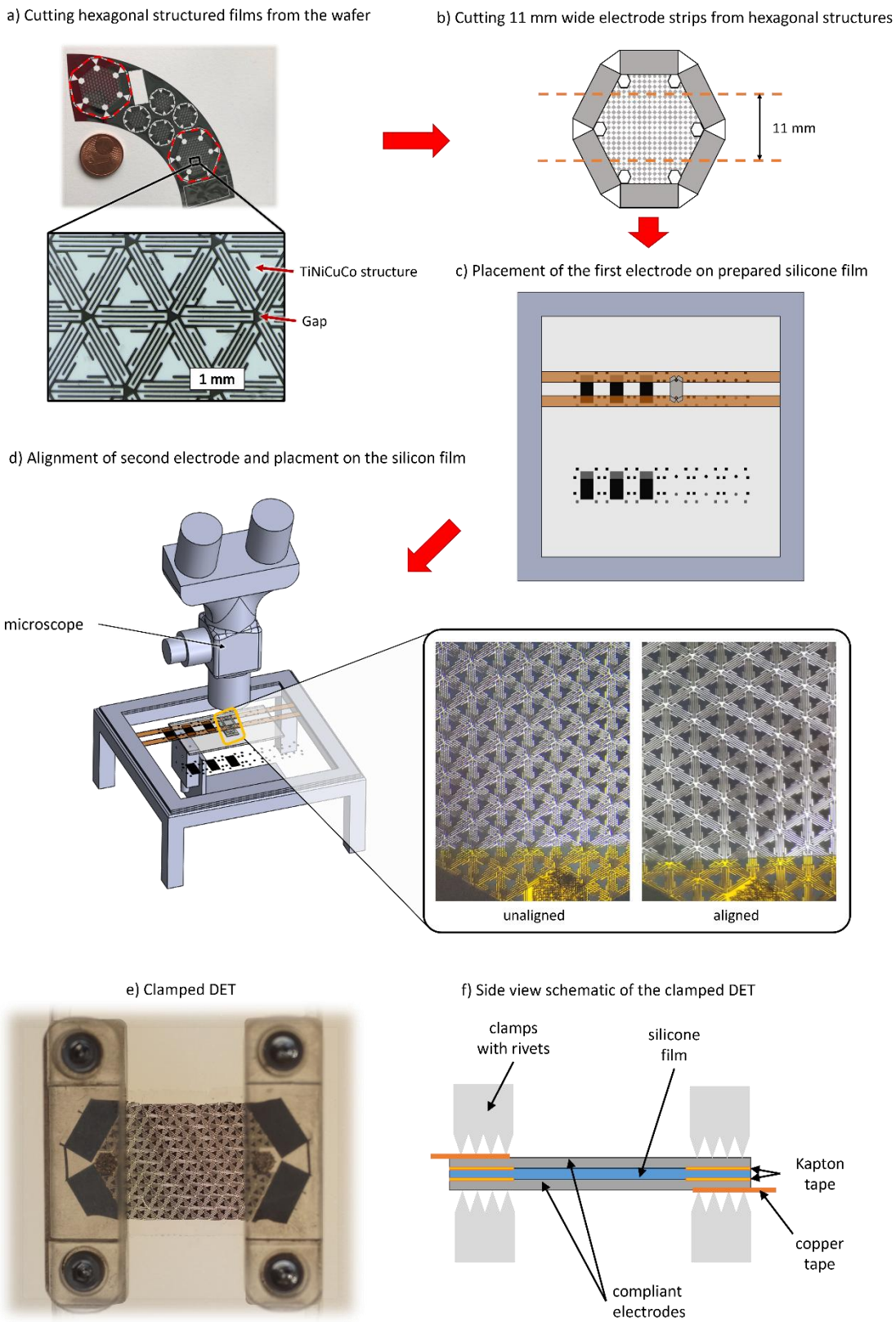

Figure 1: Preparation process of the TiNiCuCo transducers

Experimental Set-Up and Analysis

Figure 2 shows a schematic of the general experimental set-up. The samples are secured using custom 3D-printed clamps. Rivets on the clamps increase local pressure to ensure a secure fixture and to enable copper foil contacts to penetrate the titanium oxide layer on the surface of the TiNiCuCo electrodes. One clamp is fixed to an ME KD24s ±2N load cell, while the other is attached to the driving shaft of an Aerotech ANT-25LA linear actuator. For the experiments shown in this paper the load cell is not used. Displacement is measured with a Keyence LK G87 laser. Electrical connections are made using copper tape and high-voltage-capable wires. A GW Instek 8201 high-frequency LCR meter performs electrical characterization. The system is controlled via a NI LabVIEW™ environment on a Microsoft Windows host, with data acquired and synchronized by a NI cRIO™ FPGA unit. Data is stored in TDMS files and processed using MATLAB, with all graphs subjected to Gaussian smoothing (window size = 100).

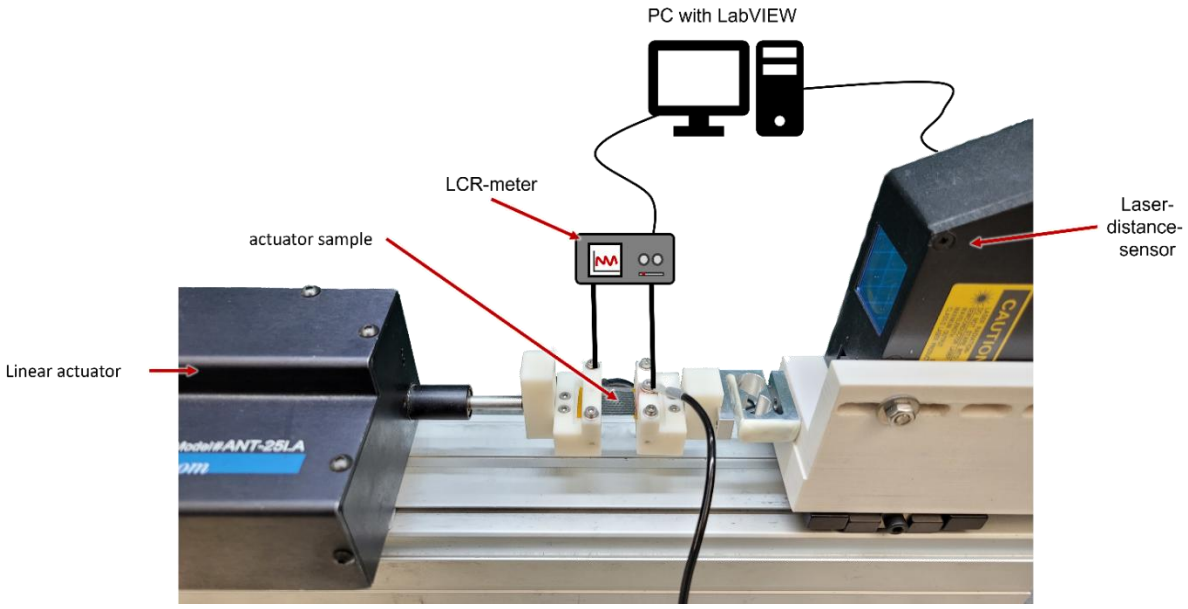

Figure 2: Experimental set-up schematic, including load cell, linear actuator, and electrical measurement components

3. RESULTS AND DISCUSSION

The integration of SSTTF electrodes with DET was evaluated based on electrical resistance and capacitance behavior while stretching the DET by 5 %. The resistance of TiNiCuCo electrodes was significantly lower than conventional CB-based electrodes. While the resistance of CB-based electrodes was measured in the order of ~10^4 Ω, the TiNiCuCo electrodes exhibited resistance values below 10 Ω, representing an improvement of more than three orders of magnitude. Figure 3a) illustrates the resistance behavior of both electrode types under applied strain. At 0 % strain, the CB-based electrodes maintained a resistance of approximately 10.4 kΩ, while the TiNiCuCo electrodes showed a resistance of only 4.56 Ω. Upon stretching to 5 % strain, the resistance of CB-based electrodes increased further due to the separation of conductive particle networks within the PDMS matrix, whereas the TiNiCuCo electrodes maintained a relatively stable resistance profile. Since the deformation of the SSTTF DET is primarily compensated by the structure and the geometry of the material itself does not change, only small resistance changes are to be expected. The low resistance and stability are crucial for high-frequency actuation, as increasing electrode resistance leads to greater power dissipation and reduced efficiency in charge transfer. The superior conductivity of the TiNiCuCo electrodes enables efficient high-frequency operation, which is essential for applications such as wearable ultrasound devices. Additionally, the low resistance allows for faster charging and discharging cycles, making these electrodes well-suited for dynamic actuation applications. Figure 3 b) and c) show the capacitance behavior of both electrode types over the time of the experiment and over the strain experienced by the DET. Measurements were performed during uniaxial strain cycles up to 5 %. For relaxed samples, PDMS+CB electrodes exhibited a capacitance of 56.9 pF, which increased to 59.7 pF at 5 % strain. The small hysteresis observed in the measurement is unexpected and is likely caused by imperfect synchronization between the measurements

of the LCR meter and the laser distance meter. The relaxed TiNiCuCo electrode samples had a capacitance of 54.6 pF, increasing to 56 pF at 5 % strain, with very narrow hysteresis. A narrow hysteresis is an important attribute for precise sensing and self-sensing. The lower overall capacitance of the SSTTF electrodes can be explained by the smaller true area, due to the structure of the electrodes. The increase in capacitance, despite the true area of the SSTTF not changing during deformation, is caused by electric field lines extending around the edges of the electrode material in the structure. This may also- in part- explain the nonlinearity of the SSTTF electrodes capacitance curve. The capacitance in conjunction with electrical resistance determines electrode charging times—a key factor in high-frequency applications. The characteristic frequency of the CB+PDMS electrodes corresponds to 270 kHz ($f = 1/2\pi RC$), whereas the TiNiCuCo electrodes exhibited a significantly lower resistance, resulting in a characteristic frequency of 635 MHz.

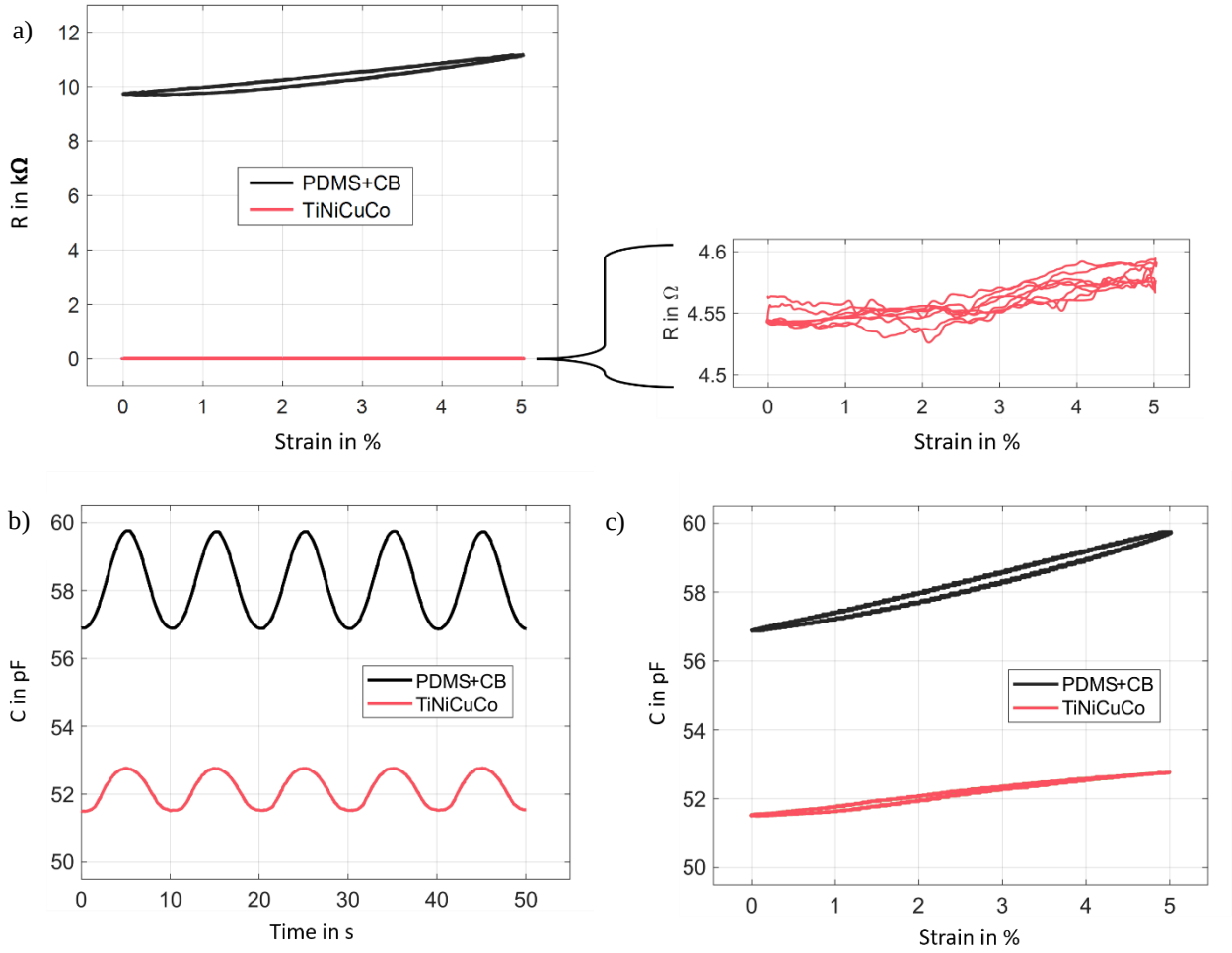

Figure 3: Experimental results: a) resistance over strain; b) capacitance over time; c) capacitance over strain

4. CONCLUSION AND OUTLOOK

The integration of freestanding, structured TiNiCuCo thin-film electrodes with DET demonstrates substantial electrical improvements over conventional PDMS+CB electrodes. Our system leverages the significantly lower resistance—yielding characteristic frequencies up to 635 MHz—and the enhanced mechanical properties of the auxetic SSTTF design. This tunable structure minimizes resistance variations during strain cycles, enabling efficient high-frequency operation that is crucial for applications such as wearable ultrasound devices [10]. Moreover, directly depositing the SMA electrodes onto the silicone film without adhesives shows a seamless interface that enhances energy transfer and maintains actuator performance under dynamic loading conditions.

The synergy between DETs and structured SMA electrodes is compelling: DETs offer large deformations and rapid actuation, while SMA electrodes provide superior conductivity, robust mechanical performance, and self-sensing through stable electrical properties. Our hybrid system, termed the shape memory alloy-based auxetic superelastic hybrid dielectric elastomer (SMASH-DE), represents a significant advancement toward multifunctional, high-performance actuators. Looking forward, experiments regarding actuation behavior, refinement of the auxetic design and the exploration of integrated biasing mechanisms are expected to improve actuation efficiency, responsiveness, and multifunctionality, paving the way for next-generation smart actuator systems.

REFERENCES

[1] I. Bezsudnov, A. Khmelnitskaya, A. Kalinina, und S. Ponomarenko, „Dielectric elastomer actuators: materials and design“, *Russian Chemical Reviews*, Bd. 92, Nr. 2, S. 5070, März 2023, doi: 10.57634/RCR5070.

[2] B. Fasolt, M. Hodgins, G. Rizzello, und S. Seelecke, „Effect of screen printing parameters on sensor and actuator performance of dielectric elastomer (DE) membranes“, *Sensors and Actuators, A: Physical*, Bd. 265, Nr. October, S. 10–19, 2017, doi: 10.1016/j.sna.2017.08.028.

[3] S. Gratz-Kelly, G. Rizzello, M. Fontana, S. Seelecke, und G. Moretti, „A Multi-Mode, Multi-Frequency Dielectric Elastomer Actuator“, *Advanced Functional Materials*, Bd. 32, Nr. 34, S. 2201889, 2022, doi: 10.1002/adfm.202201889.

[4] S. Hao *u. a.*, „A Transforming Metal Nanocomposite with Large Elastic Strain, Low Modulus, and High Strength“, *Science*, Bd. 339, Nr. 6124, S. 1191–1194, März 2013, doi: 10.1126/science.1228602.

[5] J. Mohd Jani, M. Leary, A. Subic, und M. A. Gibson, „A review of shape memory alloy research, applications and opportunities“, *Materials & Design (1980-2015)*, Bd. 56, S. 1078–1113, Apr. 2014, doi: 10.1016/j.matdes.2013.11.084.

[6] C. Chluba *u. a.*, „Ultralow-fatigue shape memory alloy films“, *Science*, Bd. 348, Nr. 6238, S. 1004–1007, Mai 2015, doi: 10.1126/science.1261164.

[7] S. M. Curtis *u. a.*, „Thin-Film Superelastic Alloys for Stretchable Electronics“, *Shap. Mem. Superelasticity*, Bd. 9, Nr. 1, S. 35–49, März 2023, doi: 10.1007/s40830-023-00422-4.

[8] S. M. Curtis, „Functionalized Thin-Film Shape Memory Alloys for Novel MEMS Applications“, 2023, Zugegriffen: 4. August 2023. [Online]. Verfügbar unter: http://hdl.handle.net/1903/30037

[9] R. Lima de Miranda, C. Zamponi, und E. Quandt, „Micropatterned Freestanding Superelastic TiNi Films“, *Advanced Engineering Materials*, Bd. 15, Nr. 1–2, Art. Nr. 1–2, 2013, doi: 10.1002/adem.201200197.

[10] C. Wang und X. Zhao, „See how your body works in real time — wearable ultrasound is on its way“, *Nature*, Bd. 630, Nr. 8018, S. 817–819, Juni 2024, doi: 10.1038/d41586-024-02066-5.